

LINK ADAPTATION IN CORRELATED ANTENNA DIVERSITY ENVIRONMENTS

Duc V. Duong, Martin Å. Wingar, and Geir E. Øien

Dept. of Electronics and Telecommunications, Norwegian University of Science and Technology
O.S. Bragstads pl. 2B, 7041 Trondheim, Norway. E-mail: {duong,oien}@iet.ntnu.no, mwingar@gmail.com.

ABSTRACT

We present results on optimization of pilot spacing and power in adaptive coded modulation (ACM) systems operating in spatially *correlated* receive antenna diversity. The analyzed ACM system has a set of multidimensional trellis codes—which are designed for Gaussian channels—to switch between. In order to switch between different modes the transmitter is provided with the channel-signal-to-noise ratio as *predicted* at the receiver. The results are presented for identically distributed Rayleigh fading subchannels with Jakes spectrum, and with 2 different correlation models: equal and exponential correlation between the antennas. Exact closed-form solutions are difficult to obtain due to the spatial correlation. Instead, approximated closed-form expressions are calculated.

1. INTRODUCTION

Quality of service (QoS) in future multimedia services can only be achieved by realizing high information rates. Thus, spectral efficient transmission schemes are called for. As opposed to the “classical” systems where the transmission is designed for and fixed to the worst channel conditions—i.e. the system is designed to perform acceptably in deep fades—the future systems also take advantages of good channel conditions. Adaptive (coded) modulation (ACM) is a promising tool to combat fading and to maximize the information rate. The idea behind an ACM system is to dynamically change rate (and power) to a mode which is more suitable to the quality of the channel, and, at the same time, maintain some QoS measure such as the target bit error rate (BER_0). In order to do such adaptation, information about channel variations must be available to the transmitter.

It is well known that pilot-symbol-assisted modulation (PSAM) can be used to track the variations of the channel, based on the fact that known symbols (pilot symbols) are inserted into the data stream at regular intervals and transmitted along with data information. These pilot symbols are extracted at the receiver and are used to perform the channel estimation and/or prediction [1]. However, uniform spacing

pilot symbols regardless of the channel quality is not necessarily optimal scheme. More pilot might be necessary when the average channel quality is bad and vice versa. However, it is obvious that too many pilot symbols will degrade system performance because much of the bandwidth is devoted to send overhead information. On the other hand, too few pilots cause inaccurate channel prediction/estimation, which would imply that the system is adapting to wrong the channel conditions, and, hence, the performance is also degraded. As a result, there should exist an optimal value which maximizes the throughput. In [2], [3] optimization schemes which adapt both pilot spacing and power allocation to the average channel signal-to-noise ratio (CSNR) in order to maximize average spectral efficiency (ASE) have been shown.

The ACM system under consideration in this paper is depicted in Fig. 1 where n_R denotes the number of receive antennas. The system has a set of N codes/constellations $\{M_n\}_{n=1}^N$ —corresponding to a set of spectral efficiencies (SEs) $\{R_n\}$ —to switch between. The code with a lower index is also of a smaller size than the one with a higher index. I.e., $M_n > M_{n-1} \forall n$, and hence $R_n > R_{n-1}$.

While it is straightforward to derive the estimation error when a linear estimator is used, we will assume now that estimation is perfect since the estimation error is very small, such that prediction error always will be the dominating factor in performance analysis. The predicted CSNR is fed back to the sender and it is called channel state information (CSI).

In order to have uncorrelated subchannels, the receive antennas must be spaced at least half the wavelength apart [4]. However, from an experimental point of view, about 10–20 wavelengths separation of the receive antennas is required to provide sufficient spatial decorrelation at the base station [5], [6]. Similarly, to provide spatial decorrelation between the antennas at the remote units, it is sufficient to separate the antennas with quarter wavelength [5].¹ Due to

¹This is due to the difference of the scattering environment around the base station and the remote station. While the remote station is usually surrounded by nearby scatterers, the base station is spaced at higher altitude with no nearby scatterers.

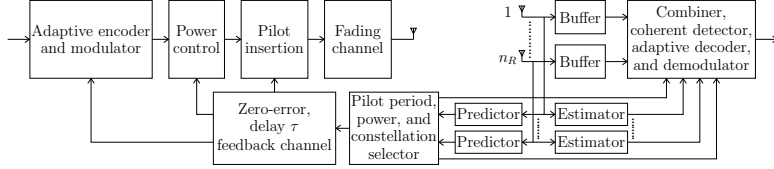


Figure 1: ACM system with multiple reception of receiving signals.

space limitations, in practical systems with antenna diversity implemented, the antennas might be spaced closed to each other. This implies that there exists some correlation between these antennas. In this paper we are going to optimize the pilot spacing and power distribution between pilot and data symbols of the ACM system (shown in Fig. 1) in the maximal ASE sense, when maximum ratio combining (MRC) is implemented and spatial correlation between different receive antennas is included. Note that the optimization algorithm used is presented in [7] and not covered in detail here.

2. SYSTEM MODEL AND THE COMBINED SIGNAL STATISTICS

With the reference to Fig. 1 the input-output relationship of the transmit data signal $s(k; l)$ and the receive data signal $y_{d;j}(k; l)$ at the j th branch can be found as

$$y_{d;j}(k; l) = \sqrt{\mathcal{E}_d} h_j(k; l) s(k; l) + n_j(k; l), \quad l \in [1, \dots, L]. \quad (1)$$

Similarly, we can write the receive pilot signal as

$$y_{pl;j}(k; 0) = \sqrt{\mathcal{E}_{pl}} h_j(k; 0) s(k; 0) + n_j(k; 0), \quad (2)$$

where the \mathcal{E}_d and \mathcal{E}_{pl} denotes the *actual* data power and the pilot power, respectively. Note that the data stream is divided into frames of L symbols where each frame starts with a pilot symbol. Thus k and l is used to index the frames and the symbols in that frame, respectively.

Based on (1), the total detected data CSNR—when assuming perfect estimation—can be calculated as

$$\gamma_d = \frac{\mathcal{E}_d \|\mathbf{h}(k; l)\|_F^2}{N_0} \quad (3)$$

where $\mathbf{h}(k; l) = [h_1(k; l), h_2(k; l), \dots, h_{n_R}(k; l)]^T$, N_0 is the noise power of the zero-mean additive white Gaussian noise (AWGN) $n_j(k; l)$. $\|\cdot\|_F^2$ and $(\cdot)^T$ denotes the Frobenious norm and vector transpose, respectively. While assuming that the channel $h_j(k; l)$ is complex Gaussian with zero mean and variance equal to 1, the total average data CSNR is $\bar{\gamma}_d = n_R \mathcal{E}_d / N_0 = \bar{\gamma}_j r_d n_R$ where $r_d = \mathcal{E}_d / \mathcal{E}$ and $\bar{\gamma}_j \triangleq \mathcal{E} / N_0$ is the average received CSNR on each branch with \mathcal{E} is the average

power each symbol (both pilot and data) is allowed to use.

We define the average predicted CSNR on one sub-channel as [3] $\hat{\gamma}_j = E[\hat{\gamma}_j] = \mathcal{E}_d E[|h_{p;j}(k; l)|^2] / N_0 = \mathcal{E}_d (1 - \sigma_{p;j}^2) / N_0$, where $h_{p;j}(k; l)$ is the predicted channel gain. Then the total average predicted CSNR will be $\hat{\gamma} = \mathcal{E}_d (1 - \sigma_p^2) n_R / N_0 = \hat{\gamma}_j r n_R$. This amounts assuming that the prediction error variance is the same on all branches, i.e., $\sigma_{p;j}^2 = \sigma_p^2 \forall j$, and $r = \mathcal{E}_d (1 - \sigma_p^2) / \mathcal{E}$. It should be mentioned that detecting the different branches independently and assuming the same prediction error variance on all branch is clearly a suboptimal scheme since the spatial correlation is not exploited. The development of an optimal scheme is a subject for further research. It is also noted that the predictor is made linear and maximum a posteriori (MAP) optimal. We refer to [1], [8, Chap. 14.2] and [2], [3] for details derivation of the predictor and calculation of the predication together with the prediction error variance $\sigma_{p;j}^2$, respectively.

When a frame of size L contains one pilot and $L - 1$ data symbols, the pilot power and the average data power is distributed as $\mathcal{E}_{pl} = (1 - \alpha)L\mathcal{E}$ and $\mathcal{E}_d = \alpha L\mathcal{E} / (L - 1)$, respectively. α is the constant which determines the power allocation between pilot and data symbols.

In rate-adaptive systems, sometimes data are not sent because the channel is predicted to be so bad that the requirement of bit error rate is not fulfilled. During that period, the transmitter continues to send pilot symbols—in order to predict the channel—and data is buffered. As a result, no data power is used during that time, and, hence, the actual data power can be set to

$$\mathcal{E}_d = \frac{\bar{\mathcal{E}}_d}{1 - \text{outage probability}} = \frac{\bar{\mathcal{E}}_d}{\int_{\hat{\gamma}_1}^{\infty} p(\hat{\gamma}) d\hat{\gamma}}. \quad (4)$$

When the branch gains (i.e., $\beta_j \triangleq |h_j(k; l)|$ and $\hat{\beta}_j \triangleq |h_{p;j}(k; l)|$) are Rayleigh distributed² and are mutually uncorrelated, both γ_d and $\hat{\gamma}$ will follow Gamma distributions [9]. In this study, however, we assume that there exists some correlation between the receiving branches. Thus, the output CSNRs are not

² x is said to have Rayleigh distribution with variance $\Omega = E[x^2]$ if the pdf of x is $p(x) \triangleq \frac{2x}{\Omega} \exp\left(-\frac{x^2}{\Omega}\right)$, $x \geq 0$.

Table 1: Parameters of the Gamma pdf of γ_d and $\hat{\gamma}$.

Correlation model	m_d	θ
Constant	$\frac{n_R}{1+\rho_s(n_R-1)}$	$\bar{\gamma}_j(1+\rho_s(n_R-1))$
Exponential	$\frac{n_R}{1+\frac{2\rho_s}{1-\rho_s}\left(1-\frac{1-\rho_s^{n_R}}{n_R(1-\rho_s)}\right)}$	$\bar{\gamma}_j\left(1+\frac{2\rho_s}{1-\rho_s}\left(1-\frac{1-\rho_s^{n_R}}{n_R(1-\rho_s)}\right)\right)$

Gamma distributed anymore [10], [11]. As a result, we can not model the correlation between γ_d and $\hat{\gamma}$ exactly. In [12] pdf for the CSNR of arbitrarily correlated Nakagami- m fading channels (Rayleigh fading if $m = 1$) is shown to be well *approximated* by a Gamma distribution, with the two first moments equal to the exact pdf. With the reference to that paper we let γ_d and $\hat{\gamma}$ be Gamma distributed with the same shape factor m_d and the scale factors θ_1 and θ_2 , respectively, and use the short hand notation $\gamma_d \sim \mathcal{G}(m_d, \theta_1)$ and $\hat{\gamma} \sim \mathcal{G}(m_d, \theta_2)$ to denote that.³ Hence the joint distribution is still described by the bivariate Gamma distribution [9], i.e., $(\gamma_d, \hat{\gamma}) \sim \mathcal{G}(m_d, \theta_1, \theta_2, \rho)$, where ρ is the correlation between γ_d and $\hat{\gamma}$:

$$\rho = \frac{\text{Cov}(\gamma_d, \hat{\gamma})}{\sqrt{\text{Var}(\gamma_d)\text{Var}(\hat{\gamma})}} = \frac{\text{Cov}(\beta^2, \hat{\beta}^2)}{\sqrt{\text{Var}(\beta^2)\text{Var}(\hat{\beta}^2)}}. \quad (5)$$

It can be shown that $\rho = |\boldsymbol{\omega}^H \mathbf{r}_p|^2 / \eta$ [13], where $\boldsymbol{\omega}$ is the vector of predictor filter coefficients and $\eta = \boldsymbol{\omega}^H \mathbf{R} \boldsymbol{\omega} + \|\boldsymbol{\omega}\|^2 / ((1-\alpha)L\bar{\gamma}_j)$. \mathbf{R}_p denotes the covariance matrix and \mathbf{r}_p is the covariance vector of the channel [7]. Note that θ_1 and θ_2 can respectively be written as $\theta_1 = r_d\theta$ and $\theta_2 = r\theta$, where θ (also m_d) is found in [13, Tab. B.1], but reproduced here in Tab. 1 for the sake of completeness. It has been shown in the same paper that the system performance with the approximated pdfs is identical or close to the performance obtained with the exact pdfs, except at very high CSNRs.

Given the power spatial correlation between any two adjacent branches as

$$\rho_s = \frac{\text{Cov}(\gamma_{d;j+1}, \gamma_{d;j})}{\sqrt{\text{Var}(\gamma_{d;j+1})\text{Var}(\gamma_{d;j})}} = \frac{\text{Cov}(\beta_{j+1}^2, \beta_j^2)}{\sqrt{\text{Var}(\beta_{j+1}^2)\text{Var}(\beta_j^2)}}, \quad (6)$$

for $j = 1, 2, \dots, n_R - 1$, the two spatial correlation models using in this paper is: (i) the constant correlation

$$\rho_{ij} = \begin{cases} 1 & \text{for } i = j \\ \rho_s & \text{for } i \neq j \end{cases}, \quad (7)$$

and (ii) the exponential correlation

$$\rho_{ij} = \rho_s^{|i-j|}, \quad (8)$$

³ x is said to be gamma distributed with shape parameter φ and scale parameter χ denoted by $x \sim \mathcal{G}(\varphi, \chi)$ if the pdf is $p(x) \triangleq \frac{x^{\varphi-1}}{\Gamma(\varphi)\chi^\varphi} \exp\left(-\frac{x}{\chi}\right)$, $x \geq 0$.

where i and j is the antenna index; $i, j \in [1, \dots, n_R]$. The exponential correlation model can be applied to an equidistant array of antenna elements, while the constant correlation model corresponds to the scenario of closely spaced receive antennas or three antennas placed on an equilateral triangle [14].

3. PERFORMANCE ANALYSIS

3.1. BER Analysis

For a given choice of code, the system is required to operate with an instantaneous BER⁴ below a pre-defined value BER₀. Thus, we need an expression for BER($M_n|\hat{\gamma}$), which can be found as

$$\text{BER}(M_n|\hat{\gamma}) = \int_0^\infty \text{BER}(M_n|\gamma)p(\gamma|\hat{\gamma})d\gamma \quad (9)$$

where

$$\text{BER}(M_n|\gamma) = \sum_{\ell=1}^{\mathcal{L}} a_n(\ell) \exp\left(-\frac{b_n(\ell)}{M_n}\gamma\right) \quad (10)$$

is the expression obtained by curve fitting to the simulated BER performance of trellis codes over AWGN channels. Unlike in [15], where the approximation expression—for high CSNR only—contains just one exponential function, we use \mathcal{L} of them to match to the simulated values over the whole range of instantaneous CSNR. The code-dependent constants $a_n(\ell)$ and $b_n(\ell)$ are found as the result of curve fitting. Those constants, and illustration of the approximation, are to be found in [7].

The instantaneous CSNR is given by (3). Replacing γ in (9) and (10) by γ_d and using the relation $p(\gamma_d|\hat{\gamma}) = p(\gamma_d, \hat{\gamma})/p(\hat{\gamma})$, BER($M_n|\hat{\gamma}$) can be found as

$$\text{BER}(M_n|\hat{\gamma}) = \sum_{\ell=1}^{\mathcal{L}} a_n(\ell) \left(\frac{M_n}{\Phi}\right)^{m_d} \exp\left(-\hat{\gamma} \frac{\rho\theta_1 b_n(\ell)}{\theta_2 \Phi}\right) \quad (11)$$

where $\Phi = M_n + b_n(\ell)\theta_1(1-\rho)$. The switching thresholds $\{\hat{\gamma}_n\}_{n=1}^N$ are found by equating (11) to the level BER₀ and solving for $\hat{\gamma}$ for different constellation sizes M_n . A numerical search must be used here.

An estimate of the average BER over all codes is given by the average number of bits in error divided

⁴instantaneous with respect to the predicted CSNR.

by the average number of bits transmitted in total [16]:

$$\text{BER} = \frac{\sum_{n=1}^N \text{BER}(M_n) P_n}{\sum_{n=1}^N R_n P_n}, \quad (12)$$

where $\text{BER}(M_n) = \int_{\hat{\gamma}_n}^{\hat{\gamma}_{n+1}} \text{BER}(M_n|\hat{\gamma}) d\hat{\gamma}$ and is

$$\begin{aligned} \text{BER}(M_n) &= \sum_{\ell=1}^{\mathcal{L}} a_n(\ell) \left(\frac{M_n}{M_n + b_n(\ell)\theta_1} \right)^{m_d} \\ &\times \left\{ \bar{\Gamma} \left(m_d, \hat{\gamma}_n \frac{M_n + b_n(\ell)\theta_1}{\theta_2\Phi} \right) \right. \\ &\quad \left. - \bar{\Gamma} \left(m_d, \hat{\gamma}_{n+1} \frac{M_n + b_n(\ell)\theta_1}{\theta_2\Phi} \right) \right\}. \quad (13) \end{aligned}$$

R_n is the SE of the actual code, $P_n = \int_{\hat{\gamma}_n}^{\hat{\gamma}_{n+1}} p(\hat{\gamma}) d\hat{\gamma} = \bar{\Gamma}(m_d, \hat{\gamma}_n/\theta_2) - \bar{\Gamma}(m_d, \hat{\gamma}_{n+1}/\theta_2)$ is the probability that the predicted CSNR falls into the region $[\hat{\gamma}_n, \hat{\gamma}_{n+1}]$,⁵ i.e., the probability that the constellation M_n is used.

3.2. ASE Analysis

The SE R_n for the code M_n when using $2G$ -dimensional trellis codes is given by [15] $R_n = (1 - 1/L)(\log_2(M_n) - 1/G)$.⁶ Hence, given R_n and P_n the average spectral efficiency is expressible as

$$\begin{aligned} \text{ASE} &= \sum_{n=1}^N R_n P_n = \frac{L-1}{L} \sum_{n=1}^N \left(\log_2(M_n) - \frac{1}{G} \right) \\ &\times \left\{ \bar{\Gamma} \left(m_d, \frac{\hat{\gamma}_n}{\theta_2} \right) - \bar{\Gamma} \left(m_d, \frac{\hat{\gamma}_{n+1}}{\theta_2} \right) \right\} \quad (14) \end{aligned}$$

When using Nyquist sampling, L must be less than $L_{\max} = \lceil 1/(2f_d T_s) \rceil$ [3] where f_d is the maximum Doppler shift. Thus, for $L \in [2, \dots, L_{\max}]$ we have the following optimization problem:

$$\begin{aligned} &\max_{\alpha, L} \text{ASE} \\ &\text{subject to } 0 < \alpha < 1. \quad (15) \end{aligned}$$

The optimization algorithm is presented in [7]. Thus we choose not to reproduce it here, but, instead, refer to that paper.

4. NUMERICAL EXAMPLE

Illustrated here is an example ACM system which has a set of $N = 8$ QAM signal constellations of sizes $\{M_n\} = \{4, 8, 16, 32, 64, 128, 256, 512\}$ to switch between. These constellations are used to represent

⁵ $\bar{\Gamma}(a, b) \triangleq \Gamma(a, b)/\Gamma(a)$ is the normalized incomplete gamma function [7].

⁶ $G = 2$ is utilized in the numerical example in Section 4.

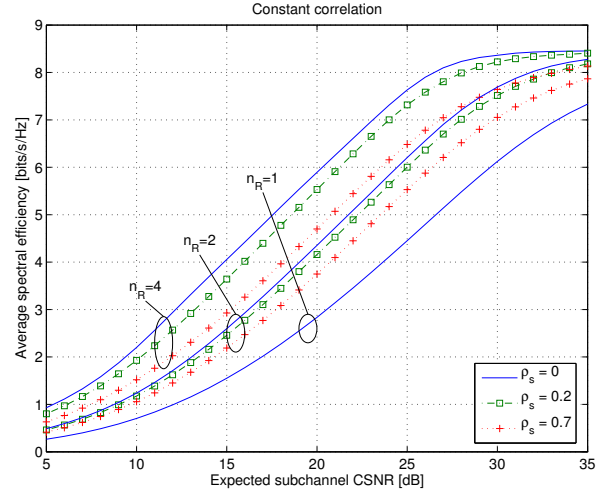


Figure 2: ASE as a function of subchannel CSNR for optimal L and optimal power allocation. The correlation between every subchannels is the same and is equal to $\rho_s = 0, 0.2, \text{ and } 0.7$, respectively.

eight 4-dimensional trellis codes [15]. The carrier frequency is 2 GHz and the length of a channel symbol is 5 μs —corresponding to a channel bandwidth of 200 kHz using Nyquist sampling. The mobile velocity is $v = 30$ m/s and the system delay considered is $\tau = 1$ ms (meaning that we predict 1 ms ahead in time). With these parameters, the Doppler frequency is $f_d = 200$ Hz and the normalized delay $\tau f_d = 0.2$. We require the system to tolerate an $\text{BER}_0 = 10^{-5}$, and we choose the order of the predictor to be $K_p = 250$. Furthermore, we assume that the expected subchannel CSNR is the same for all the branches—i.e., $\bar{\gamma} = \{\bar{\gamma}_j\}, \forall j \in \{1, \dots, n_R\}$ where n_R is the number of receive antennas—and that they are correlated either with equal correlation factor, or with exponential correlation factor. Note also that since $\tau = DLT_s = 1$ ms, the pilot spacing L is in $\{2, 4, 5, 8, 10, 20, 25, 40, 50, 100, 200\}$.

We see from Figs. 2 and 5 that ASE is reduced with increasing spatial correlation between the available antennas. This is due to the fact that the diversity gain becomes smaller with larger spatial correlation. Moreover, constant correlation causes more performance degradation than exponential correlation. This is due to the fact that, in the latter case, the correlation between one antenna with the other antennas decreases exponentially with distance between them, while the correlation is the same between any two antenna branches in the former case. The performance is identical—for both cases—when $n_R = 2$.

When all the branches are fully correlated with each other, the diversity gain will disappear. This implies that increasing the spatial correlation will affect both

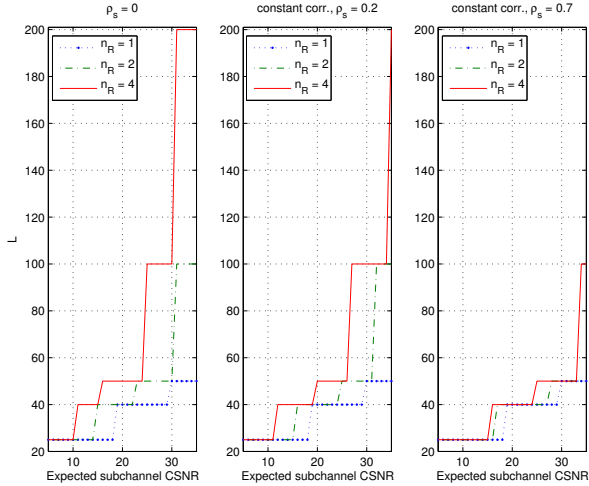


Figure 3: Optimal pilot spacing with equal correlation for $\rho_s = 0, 0.2$, and 0.7 , respectively.

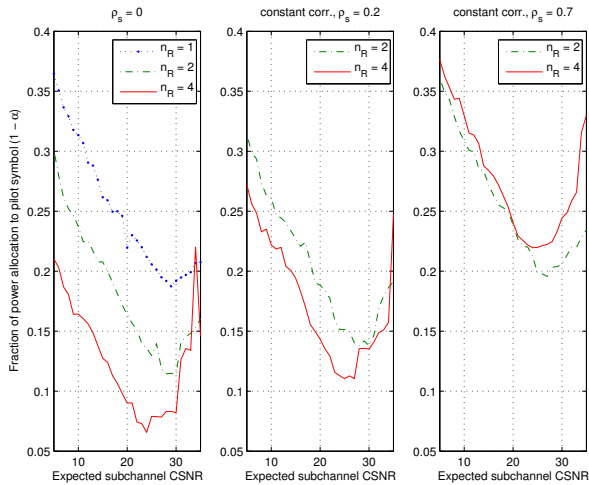


Figure 4: Optimal pilot power with equal correlation for $\rho_s = 0, 0.2$, and 0.7 , respectively.

the pilot insertion frequency and the power allocation to pilot symbol in the way that it approaches the non-diversity case ($n_R = 1$), and this is shown in Figs. 3, 4, 6, and 7. At very high CSNR the pilot power increases again. This can be explained the fact by that pilot spacing L jumps to a very high value at the same point—meaning that pilot symbols are seldom transmitted. Since the system is relying on the accuracy of the prediction of the channel, more power should be put on pilots such that the quality of the prediction is maintained (hence, the BER performance is maintained).

Shown in Fig. 8 is the theoretical average BER performance (evaluated from Eq. (12)) with constant correlation model and different values of correlation ρ_s . It is plotted for optimal values of pilot spacing and op-

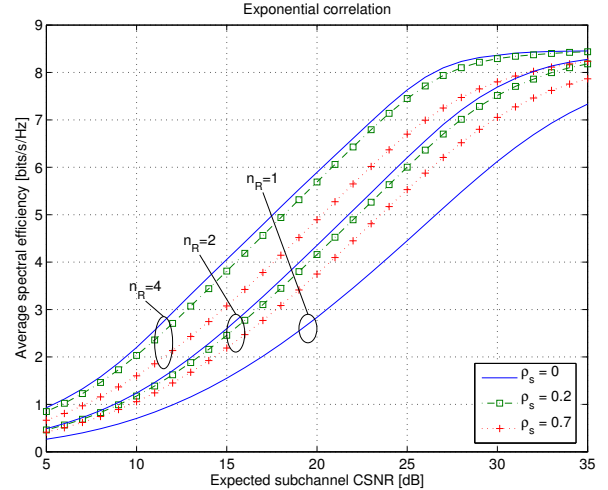


Figure 5: ASE as a function of subchannel CSNR for optimal L and optimal power allocation. The correlation between every subchannels is reduced exponentially with the distance between the antennas and $\rho_s = 0, 0.2$, and 0.7 , respectively.

timal power allocation. The conclusion here is that average BER is always below the requirement of 10^{-5} . Similarly, BER performance is also satisfied with the exponential correlation model.

5. CONCLUSIONS

We have illustrated how the spatial correlation would affect the performance of a certain rate-adaptive system having receive antenna diversity implemented. The throughput in terms of ASE is reduced due to the reducing diversity gain when spatial correlation increases. The performance degradation is larger with constant correlation compares to with exponential correlation when the numbers of receive antenna is greater than 2.

The detection scheme and the optimization approach are however suboptimal since they do not take into account the fact that the subchannels are correlated. This problem might be solved by deriving a joint detection and optimization algorithm for all the branches, and this is subject to further research.

6. REFERENCES

- [1] J. K. Cavers, "An analysis of pilot symbol assisted modulation for Rayleigh fading channels," *IEEE Transactions on Vehicular Technology*, vol. 40, no. 4, pp. 686–693, Nov 1991.
- [2] D. V. Duong, G. E. Øien, and K. J. Hole, "Adaptive coded modulation with receive antenna diversity and imperfect channel knowledge at receiver and transmitter," in *Proc. European Signal Processing Conference (EUSIPCO)*, Antalya, Turkey, Sept 2005.

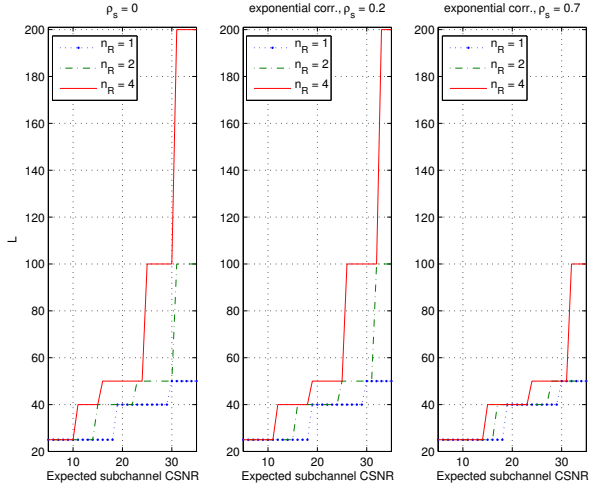


Figure 6: Optimal pilot spacing with exponential correlation for $\rho_s = 0, 0.2, \text{ and } 0.7$, respectively.

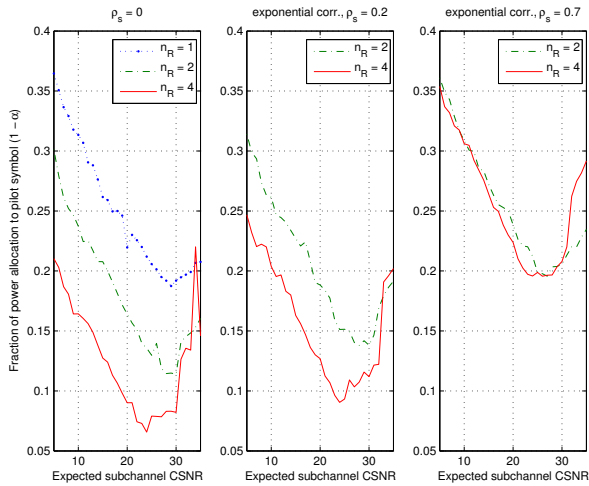


Figure 7: Optimal pilot power with exponential correlation for $\rho_s = 0, 0.2, \text{ and } 0.7$, respectively.

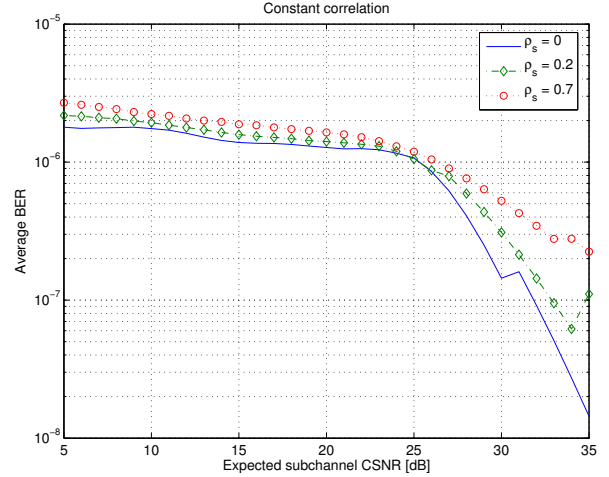


Figure 8: Average BER with equal correlation model, optimal pilot spacing, and optimal power allocation as a function of expected subchannel CSNR for different correlation ρ_s .

- [3] X. Cai and G. B. Giannakis, "Adaptive PSAM accounting for channel estimation and prediction errors," *IEEE Transactions on Wireless Communications*, vol. 4, no. 1, pp. 246–256, Jan 2005.
- [4] T. S. Rappaport, *Wireless Communications Principles & Practice*. Prentice Hall, 1999.
- [5] J. H. Winters, "Smart antennas for wireless systems," *IEEE Personal Communications*, vol. 5, pp. 23–27, Feb 1998.
- [6] S. M. Alamouti, "A simple transmit diversity technique for wireless communications," *IEEE Journal on Selected Areas in Communications*, vol. 16, no. 8, pp. 1451–1458, Oct 1998.
- [7] D. V. Duong, G. E. Øien, and K. J. Hole, "Adaptive coded modulation with receive antenna diversity and imperfect channel knowledge at receiver and transmitter," accepted for publication in *IEEE Transactions on Vehicular Technology*. Available at www.tele.ntnu.no/users/duong/publications/vt-18052005.pdf.
- [8] H. Meyr, M. Moeneclaey, and S. A. Fechtel, *Digital Communication Receivers: Synchronization, Channel Estimation and Signal Processing*. John Wiley & Sons, 1998.
- [9] G. E. Øien, H. Holm, and K. J. Hole, "Impact of channel prediction on adaptive coded modulation performance in Rayleigh fading," *IEEE Transactions on Vehicular Technology*, vol. 53, no. 3, pp. 758–769, May 2004.
- [10] V. A. Aalo, "Performance of maximal-ratio diversity systems in a correlated Nakagami-fading environment," *IEEE Transactions on Communications*, vol. 43, no. 8, pp. 2360–2369, Aug 1995.
- [11] M.-S. Alouini, A. Abdi, and M. Kaveh, "Sum of gamma variates and performance of wireless communication systems over Nakagami-fading channels," *IEEE Transactions on Vehicular Technology*, vol. 50, no. 6, pp. 1471–1480, Nov 2001.
- [12] C. Mun, C.-H. Kang, and H.-K. Park, "Approximation of SNR statistics for MRC diversity systems in arbitrarily correlated Nakagami fading channels," *Electronics Letters*, vol. 35, no. 4, pp. 266–267, Feb 1999.
- [13] B. Holter, "Adaptive coded modulation in spatial and multi-user diversity systems," Ph.D. dissertation, Norwegian University of Science and Technology, 2005.
- [14] M. K. Simon and M.-S. Alouini, *Digital Communication over Fading Channels: A Unified Approach to Performance Analysis*, 2nd ed. John Wiley & Sons Inc., 2005.
- [15] K. J. Hole, H. Holm, and G. E. Øien, "Adaptive multi-dimensional coded modulation over flat fading channels," *IEEE Journal on Selected Areas in Communications*, vol. 18, no. 7, pp. 1153–1158, July 2000.
- [16] M.-S. Alouini and A. J. Goldsmith, "Adaptive modulation over Nakagami fading channels," *Kluwer J. Wireless Communications*, vol. 13, pp. 119–143, May 2000.